AJP

ISSN : 0971 - 3093

Vol 34, Nos 3 & 4, March-April, 2025

ASIAN JOURNAL OF PHYSICS

An International Peer Reviewed Research Journal

P K Kaw Memorial Issue

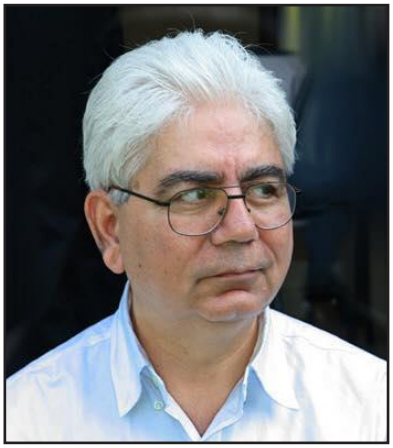

Prof P K Kaw

Guest Editors : Ramesh Narayanan & Satyananda Kar

ap

ANITA PUBLICATIONS

FF-43, 1st Floor, Mangal Bazar, Laxmi Nagar, Delhi-110 092, India

B O : 2, Pasha Court, Williamsville, New York-14221-1776, USA

Asian Journal of Physics
Vol. 34, Nos 3 & 4 (2025) 211-222
Available on: www.asianjournalofphysics.com

ap

Hydrogen plasma characterization in an ECR based large volume plasma source under different cusp magnetic field topologies

Bibekananda Naik[1], S Sharma[1], R Narayanan[1], D Sahu[1], M Bandyopadhyay[2,3], A Chakraborty[2], M J Singh[2,3], R D Tarey[1] and A Ganguli[1]

[1]*Indian Institute of Technology Delhi, Hauz Khas, New Delhi, Delhi-110 016, India*

[2]*Institute for Plasma Research, Gandhinagar- 382 428, Gujarat, India*

[3]*Homi Bhabha National Institute, Mumbai, Maharashtra 400 094, India*

Dedicated to Prof P K Kaw

Extraction of ions from hydrogen plasma is useful for several applications such as ion sources for high energy linear particle accelerators, neutron generation, tandem accelerator, accelerator based mass spectrometry, plasma thrusters for space application, microelectronics etching and most importantly in fusion science for heating and diagnosis of thermonuclear fusion plasmas. A few important desirable characteristics of the plasma source are high plasma density (~10^{10} - 10^{12} cm^{-3}), good plasma uniformity (1-5%), high system efficiencies in terms of energy consumption and in some cases moderately large volume (~m^3) plasmas. Plasma Lab, IIT Delhi developed a large volume plasma source which could produce uniform plasma of density ~ 10^{10} cm^{-3} over an area of diameter ~ 1m at a distance of ~ 37.5 cm from the source mouth. This paper reports the further investigations carried out in this system to augment the hydrogen plasma density under various magnetic cusp topologies and find a conducive condition for H- generation. The plasma was produced using a compact ECR microwave plasma source (cylindrical, diameter Φ = 91 mm and length, l = 110 mm) mounted onto the top dome of the chamber and was allowed to expand into a cylindrical expansion chamber having height as well as diameter of 1m. The magnetic field generated from the permanent NdFeB magnets used in the source section has its field strength decaying exponentially into the plasma expansion chamber. In addition to the source magnets, additional permanent ring magnets (4 Nos) were mounted onto the periphery of the cylindrical surface to aid better confinement of plasma in the central region of the chamber reducing plasma loss to the chamber wall. Two different configurations were explored, Configuration A: Adjacent magnets with opposite polarity & Configuration B: All magnets with same polarity as that of the top source facing the plasma. The plasma was characterized using Langmuir probes fabricated in house. Results at 1-3 mTorr gas pressure and microwave power (300-600W) indicate similar plasma density with reduced uniformity in configuration A, whereas enhanced plasma density (n_i ~ 10^{11} cm^{-3}) with low electron temperature (1-2 eV) was obtained for configuration B. However, the plasma uniformity was affected due to the disturbed azimuthal symmetry of the system imposed by sidewall magnets.

doi: 10.54955/AJP.34.3-4.2025.211-222

Keywords: Hydrogen plasma, Magnetic confinement, Large volume plasmas, ECR plasma,, Langmuir probe.

1 Introduction

Hydrogen plasmas are rich in various active species, including molecular hydrogen (H_2), atomic hydrogen (H), protons (H^+), molecular ions (H_2^+), triatomic hydrogen ions (H_3^+), and even negative hydrogen ions (H^-) along with hydrogen radicals (H, 2H). The presence of these species endows hydrogen plasma with

Corresponding authors
e mail:bibekanandanaik.fm@gmail.com (*Bibekananda Naik*), *rams@dese.iitd.ac.in* (*Ramesh Narayanan*), *dpsahu@dese.iitd.ac.in* (*Debaprasad Sahu*)

unique physical and chemical properties, allowing it to be used effectively across numerous applications promoting research and developments in the field of hydrogen plasmas worldwide. Two major utilizations of hydrogen plasmas are found in the area of plasma based material processing and production of ion beams (H^+, H^-) for various applications. Hydrogen plasmas are utilized for the removal of impurities from metals or semiconductor surfaces where impurities get removed in the form of water or hydrocarbons or oxides which are produced after chemical reactions with hydrogen atoms supplied by plasma [1,2]. They are also used in the passivation of semiconductor material to stabilize it from damage and to enhance the electronic properties of the material [3]. Hydrogen activation technology based on electron attachment for fluxless soldering at ambient pressure and normal soldering temperature using mixtures of hydrogen in nitrogen has advantages over conventional techniques [4]. It has also been established that high quality diamond films are grown in hydrogen diluted plasma, and that the atomic hydrogen present in these plasmas is essential for the quality of the films [5]. Atomic hydrogen sources are also being utilized for surface treatment of archaeological artefacts to protect them from post corrosion without inducing any surface damage [6]. Plasma based ion beam production and its extraction is a continually evolving field due wide range of applications of the extracted ion beams. Hydrogen plasma is a source to both positive (H^+, H_2^+, H_3^+) and negative (H^-) ions which are utilized in the field of particle accelerators [7], ion implanters, focused ion beams [8], ion projection lithography [9], accelerator based mass spectrometry [10], plasma thrusters for space application [11], microelectronics etching [12] and most importantly in fusion science for heating and diagnosis of thermonuclear fusion plasmas [13]. In thermonuclear fusion, H- ions produced in hydrogen plasma are extracted for the production of high energy neutral beams that are injected into the plasma core where they deposit their energy to the plasma species raising their temperature and helping to achieve the condition required for significant thermonuclear fusion reactions [14]. Hydrogen ion beams are also used as diagnostic neutral beam (DNB) for the measurement of helium ash density in the core of fusion plasma chamber [15]. Figure 1 summarizes all these aforementioned applications of hydrogen plasmas.

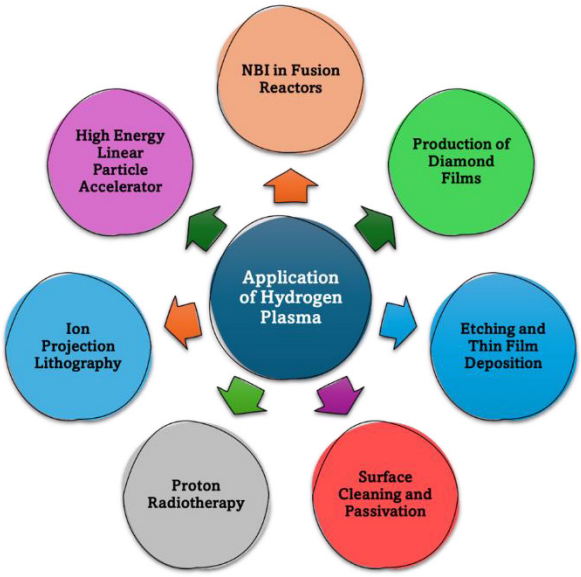

Fig 1. Applications of hydrogen plasma.

In the field of plasma based material processing, the desired properties of hydrogen plasma include high ion densities for process efficiency, tailored ion energies for precision control and minimizing damage,

controlled electron temperature for consistent plasma behaviour and controlled reactivity, presence of reactive species, low impurity levels, uniform plasma distribution for even processing, low-pressure operation and controlled plasma potential influencing particle flux onto the substrate. These properties enable hydrogen plasma to be versatile in material processing applications. Although plasma systems for each application have to meet specifications that are peculiar to the latter, few important things desirable are high plasma density (~10^{10}-10^{12} cm^{-3}), good plasma uniformity (1-5%), high system efficiencies and in some cases moderately large volume (~m^3) plasmas. Hydrogen plasma production for fusion applications have even more challenging requirements of plasma parameters. To realize thermonuclear fusion, an International Thermonuclear Experimental Reactor (ITER) is currently being built at Cadarache, France. ITER, with the aim of achieving a power amplification factor (Q) of 10, comprising of a set of two Neutral Beam Injectors with 17 MW input power per beam line and a pulse length of 3600 sec. These NBI systems are based on neutralization of H- ion beams which has beam current of ~ 45 A accelerated up to 1 MeV energy. In order to extract H- current densities ~ 30 - 35 mA/cm^2, one requires plasma density, n ~10^{12} cm^{-3} and T_e ~ 1 eV in front of the extraction grid with ~ 5 - 10 % uniformity across a large area (~ 2.0 m × 0.6 m) [14]. ITER will also feature a DNB system based on H^- ions, operating at a current of 60 A and 100 keV energy [15].

If one talks about hydrogen plasma sources and the desired plasma parameters for the above mentioned applications, one of the most important factors comes out to be the plasma production mechanism in these sources which greatly influences the produced plasma parameters. Electron Cyclotron Resonance (ECR) mechanism is known to be one of the most efficient methods for production of plasmas as they incorporate collision less heating leading to significant plasma parameters with expense of very less power when compared to other conventional plasma sources like DC & RF discharges. Some of the characteristics of ECR plasmas are high plasma density, low working pressure, low plasma potential and high ionization efficiency [16]. ECR sources are generally operated at low gas pressures that results in reduced ion collisionality in the substrate sheaths necessary for anisotropic etching. Higher plasma density implies higher ion fluxes onto the substrate important for higher processing rate and also advantageous for operating with nonpassivating chemistries. Low plasma potential helps in reducing physical damage to the substrates from ion bombardment as well as reducing unwanted sputtering of deposited materials. They also provide independent control of ion energy and ion flux with localized microwave power absorption which have significant advantages in processing applications. Talking about fusion applications of hydrogen plasma produced ion beams, current technologies utilized by the fusion community involve radio frequency (rf) input power ~ 1 MW in inductively coupled plasma (ICP) mode [17]. It can be presumed that the power coupling efficiency in rf plasma systems are collision-based, which is not so efficient as compared to plasma systems with resonant power coupling. In this regard, ECR mechanism is known to be a more efficient mechanism in terms of power coupling than ICPs but has remained relatively unexplored for such large area, high current sources due to various scientific and technological complexities associated with it. Plasma Lab IIT Delhi (PL: IITD) has been actively pursuing research in the field of ECR-based large-volume plasma sources and their characterization for the past few decades. These efforts were initiated with the development of a light-weight Compact ECR Plasma Source (CEPS) [18], weighing only 14 kg including the magnets, magnetron, triple stub tuner and plasma source chamber. Past results achieved utilizing a single CEPS, are in moderately good range with uniformity ($\Delta n/n$) ≈ 10 %, hydrogen plasma density (n_0) ~ (1 – 5)×10^{16} m^{-3} and bulk electron temperature (T_e) ~1 – 2 eV across 0.3 – 0.5 m radius in the pressure range ≈ 2 – 3 mTorr with input microwave power of ~ 0.5 – 1 kW [19]. This paper reports the further investigations carried out in a large volume plasma system to augment the hydrogen plasma density under various magnetic cusp topologies for utilizations in earlier mentioned applications and large area uniform H-production.

This paper is divided into four sections for the accessibility of the reader. Section 2 gives the description of the experimental system along with the compact ECR plasma source (CEPS). The inhouse

fabrication and working principle of the Langmuir probe is also presented in this section. Since magnetic field plays an important role in plasma confinement, the CEPS source and different chamber magnetic field configurations employed are explained in Section 3. Results obtained in terms of Langmuir probe measurements under various operating experimental conditions are presented in Section 4. Finally, in Section 5 the paper concludes with significant outcomes of the work in terms of characterizations of ECR produced hydrogen plasma which can be explored further to utilize this compact source as a potential candidate for large area H- production for fusion applications.

2 Experimental Setup and Diagnostics

The schematic diagram of the experimental setup used for the study is shown in Fig 2. It consists of a cylindrical stainless steel chamber (Diameter/Height ~ 1 m) made up of a no. of cylindrical sections with necessary ports for mounting plasma sources and diagnostics that are stacked one upon the other. The top dome of the chamber is equipped with seven ports (ID ≈ 91 mm) with a central one and the remaining six placed symmetrically on a circle. It is also provided with additional ISO KF type ports for plasma diagnostics. The bottom dome is supplied with a central port to which a diffusion pump (Varian Make, VHS-6 with standard cold cap) is adapted and is backed by a mechanical rotary vane pump (Varian Make, DS 1002) that evacuates the chamber down to a base pressure of 5×10^{6} Torr that is monitored with the help of an ionization gauge (Agilent make, inverted magnetron type XGS 800). Grade 1 Hydrogen gas (IS 1090) introduced into the chamber is controlled via a precession needle valve. The working pressure which ranges typically 1-3 mTorr in this study is monitored with the help of an MKS Baratron type 626 pressure transducer with a full range of 0.01 Torr and MKS series 600 pressure controllers. The plasma is sustained by the plasma source CEPS, a patented product of Plasma Lab: IIT Delhi [20] is mounted onto the central port of the top dome. This indigenously developed compact plasma source consists of a SS cylindrical plasma source chamber of length 110 mm and diameter 91 mm which is water cooled. The source assembly consists of a cavity magnetron for microwave generation, a waveguide section, a triple stub tuner for load matching, rectangular to circular waveguide transition along with a coaxially mounted three concentric NdFeB permanent ring magnets (Brown in Fig 2) providing an exponentially decaying diverging field into the larger expansion chamber that helps plasma flow. The ECR surface (B ~ 875 G, corresponding to 2.45 GHz) lies inside the source chamber and is quite complex. Detailed explanation of the CEPS can be found elsewhere [18]. The source is operated by a microwave power supply (2.45 GHz) with a power range of 0.3-1.0 kW and are air cooled. The impedance matching through triple stub tuner is manually optimized to reduce reflected microwave power that is monitored with the help of a power sensor (Agilent Make, U2000A). A more comprehensive description of the source and chamber magnetic field under different configurations are presented in the next section.

Plasma is characterized with the help of inhouse fabricated Langmuir probes (LP) that are introduced from the top and sidewall of the chamber. Each probe is made up of a tungsten tip of diameter ~0.25 mm with a length of few mm. In the current study the L-shaped Langmuir probe (LP-1) is used for both axial as well as radial measurements and is inserted from the top dome with a tip length of 5.1 mm. The tip of the probe is oriented radially i. e. perpendicular to the z- axis of the chamber, z = 0 being the centre of the top dome inner surface. For radial measurements, two LP was inserted at z = 37.5 cm, one along the sidewall magnets (RLP-1) and the other in between two magnets (RLP-2) as can be seen in Fig 2. Talking about the construction of the probe, the tungsten tip is inserted into a needle for electrical connection which at the other end is connected to a conducting wire placed inside ceramic tube for heat insulation. The needle is housed inside a thin ceramic tube (ID 0.58 mm) which is again placed inside a thicker tube (ID 1.58 mm) with a constriction for proper alignment of the assembly. The gaps between the tubes is filled with ceramic paste with repeated baking at 300 °C. The whole assembly is placed inside an SS tube (OD 6.35

mm) designed accordingly. Figure 3 shows the schematic and the assembled Langmuir probe. Electrical biasing to the probe is applied with the help of an electrical circuit which also helps in data measurement when connected to LabVIEW through data acquisition card (DAC). The LP data thus obtained was analyzed with the help of a MATLAB code to determine plasma parameters: the bulk electron density (n_e) and its temperature (T_e), the plasma potential (V_p) and the warm electron density and its temperature (n_w, T_w).

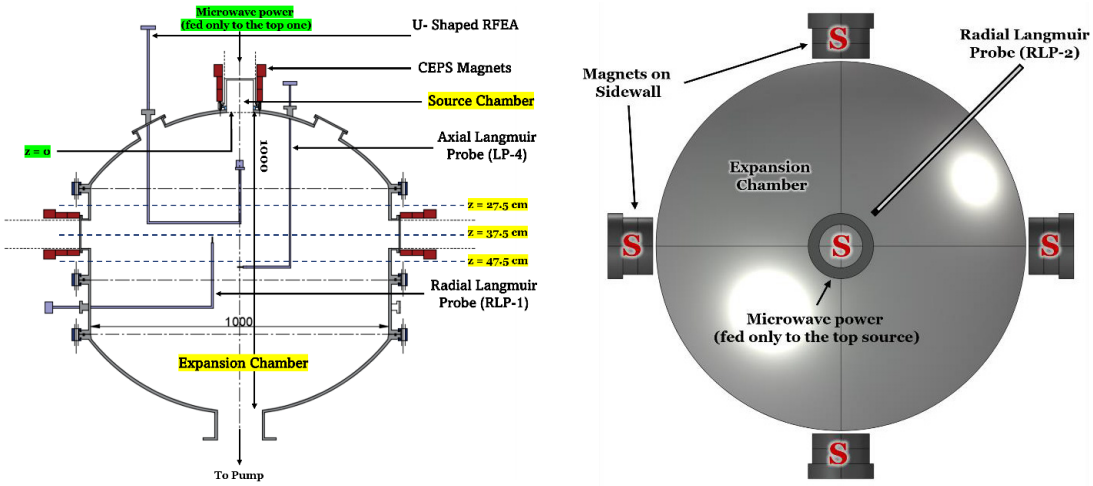

Fig 2. Schematic of vertical cross section (Left) & top view (Right) of the experimental setup.

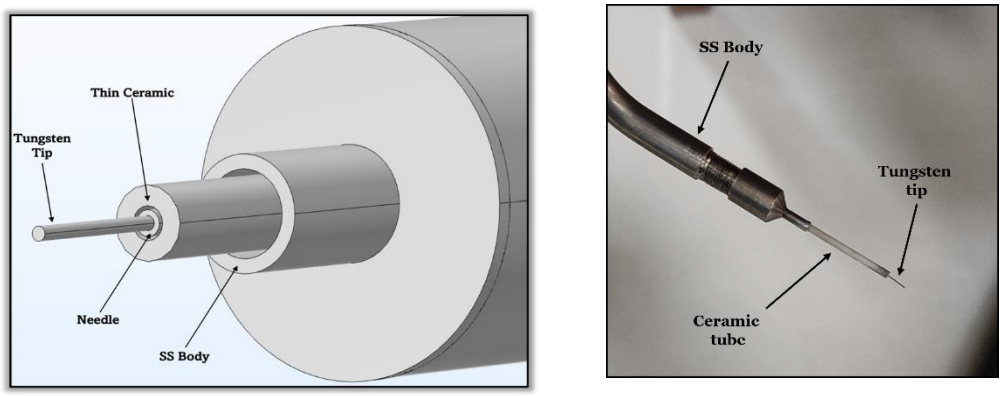

Fig 3. Schematic of Langmuir probe components (Left), Fabricated probe assembly (Right).

3 Source and chamber magnetic field configuration

As stated earlier, the CEPS source magnetic field is obtained with the help of three concentric rings magnets placed coaxially around the source chamber. In addition to it, four sets of CEPS magnets were also attached to the periphery of the expansion chamber symmetrically with different polarity giving rise to a complex magnetic field configuration inside the expansion chamber. Two different chamber magnetic field configuration is reported in this work. The simulated field configuration is presented in this section which are obtained using COMSOL Multiphysics software. Figure 4 shows the contour plot of the source magnetic field configuration which shows a single ECR layer (White contour) inside the plasma source

section corresponding to a field strength of 875 G where microwave power is coupled to the electrons through magnetic mirror action . The electrons gain sufficient energy while crossing the layer repeatedly and escape the field when they collide with the background gas by ionizing them thereby producing plasma. The axial field profile shows an exponentially decaying diverging field that helps plasma flow into the expansion chamber [21]. The four magnets are placed in the sidewall at axial distance of 37.5 cm in such a way that in configuration A, the adjacent magnets are opposite in polarity and magnets with same polarity face each other . In the second configuration B, all the magnets have the same polarity facing the plasma as that of the top source (South) as can be seen in Fig 2. It should be noted that the microwave power is fed only to the top source. The sidewall magnets forms a cusp field at the central region of the expansion chamber that reduces plasma wall losses leading to the enhancement in the plasma density. The simulated vertical cross-section and horizontal cross-section of the magnetic field configuration at z = 37.5 cm of the expansion chamber is shown in the Fig 5. Detailed experimental results in terms of plasma parameters are described in the next section.

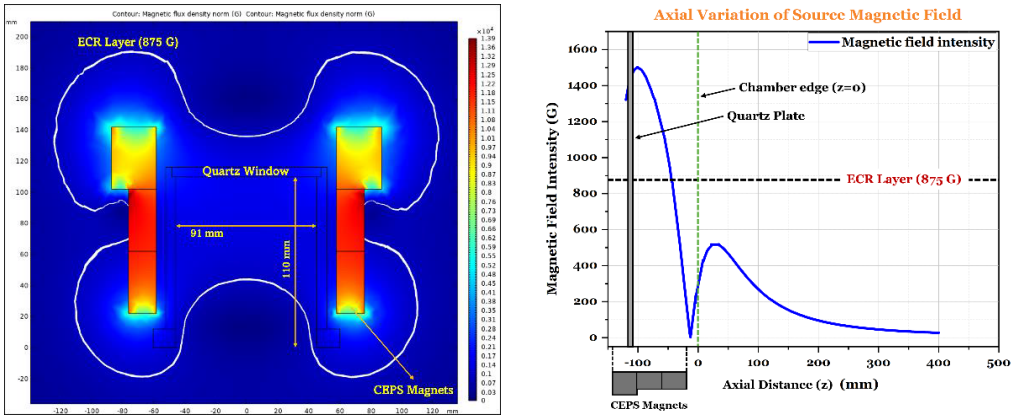

Fig 4. Contour plot of magnetic field intensity showing a single ECR layers inside the source section (Left), Axial variation of source magnetic field configuration (Right).

4 Results and Discussion

As can be seen in the Fig 5, in configuration A, where two out of four sidewall magnets facing each other has opposite polarity with respect to the magnets of the top source. So, the magnetic field lines emerging from the top magnet terminate in one of the sidewall magnet pairs, yielding in splitting of the plasma as it expands. As a result, radial non-uniformity is observed in plasma parameters. However, in second case B, due to the same polarity of the magnets facing the plasma at the sidewall, the magnetic field lines emerging from the top source are pushed towards the centre which can result in better plasma confinement and reduced plasma wall losses. Detailed experimental results under these two configurations are explained in this section. The experiments are conducted with hydrogen with the two field configurations mentioned in the previous section at 1-3 mTorr gas pressure with variable microwave power (400-600W) and the results are compared with the earlier configuration without any sidewall cusping magnets present. Axial variation of plasma parameters are measured along with the radial variations at different z planes with the help of an L-shaped LP (LP4). Radial measurements at z = 37.5 cm were carried out with the help of two radial LPs, RLP-1 & RLP-2, as stated earlier. Axial LP profiles were taken starting from 12.5 cm from the source mouth going up to z = 67.5 cm with a step of 5 cm for configuration A and a step of 2.5 cm for configuration-B. Radial profiles at three axial locations (z = 27.5 cm, 37.5 cm, 47.5 cm) were also obtained

with the same probe by rotating the probe through different angles for configuration A. The experimental results are discussed below.

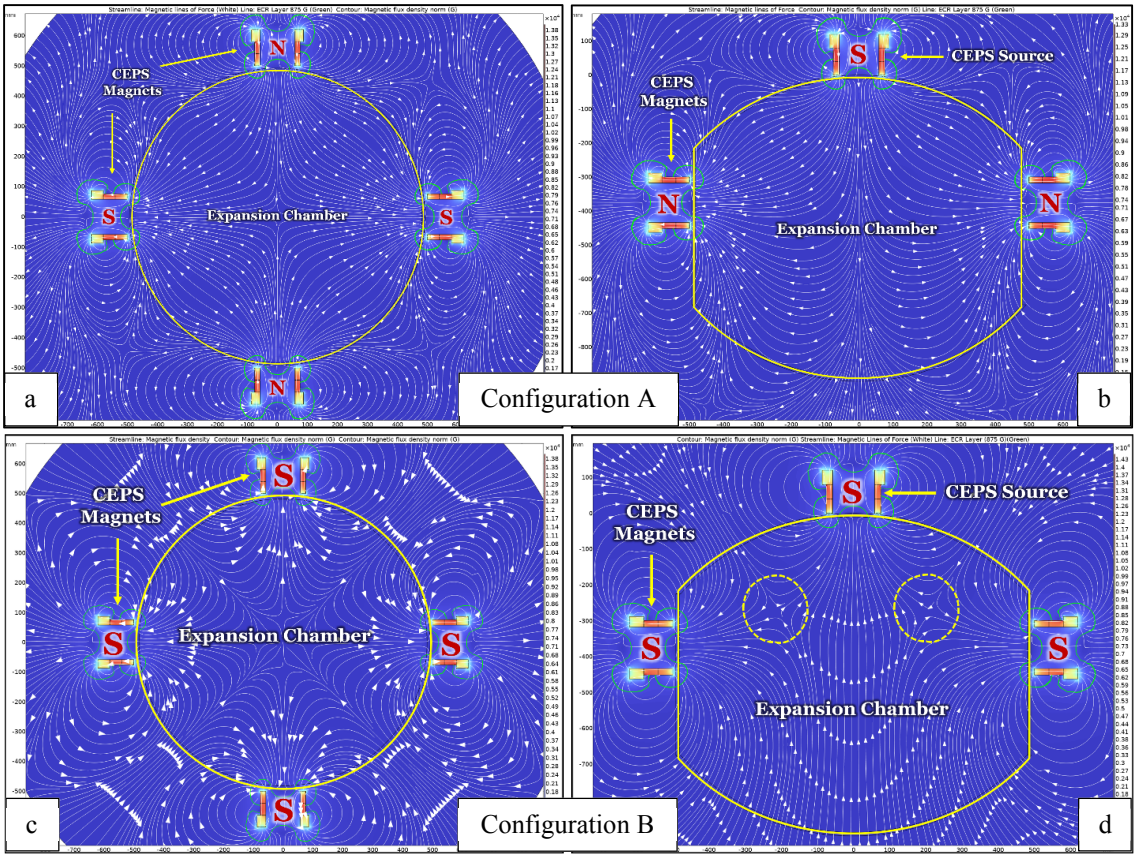

Fig 5. Simulated chamber magnetic field configuration (a) Horizontal CS at 37.5 cm, (b) Vertecal CS for configuration A and (c) Horizontal CS at 37.5 cm, (d) Vertecal CS for configuration B.

4.1 Configuration A (*Cusped field at the sidewall*)

Figure 6 shows the axial variation of plasma parameters at two different operating conditions for magnetic field configuration A. Plasma density with sidewall cusping magnetic field configuration appears to be moderately uniform over a range of 30-35 cm with a dip in density observed for 400 W for z > 50 cm , whereas uniformity goes up to z = 65 cm in case of 500 W with a reduced value. One can observe a fall in electron temperature as we move away from the source mouth reflecting the phenomenon of plasma expansion with a sharper fall for 400 W as compared to 500 W and the plot of temperature shows the same nature with axial distance as that of plasma density for z > 25 cm with a bit higher temperature for 500 W which is understandable. Plasma potential varies in the range of 5-10 V with a higher value for 500 W for most part of the axial distance. A dip in plasma potential is observed for 400 W for z > 60 cm which is opposite for 500 W. The experimental results with this configuration is also compared with the results obtained for a single CEPS source mounted onto the top dome with no additional magnets placed at the sidewall and are presented in Fig 7. Plasma density shows a fall as we move away from the source with no sidewall magnets whereas the density remains moderately uniform in the presence of sidewall cusping magnets with a comparable value.

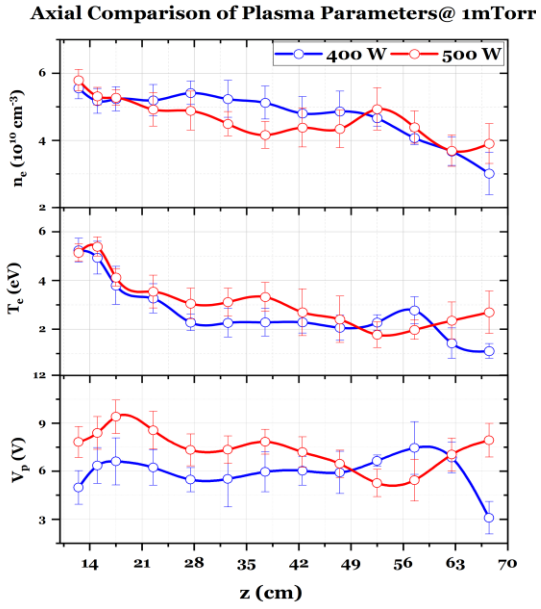

Fig 6. Axial variation of plasma parameters with sidewall magnets for configuration A.

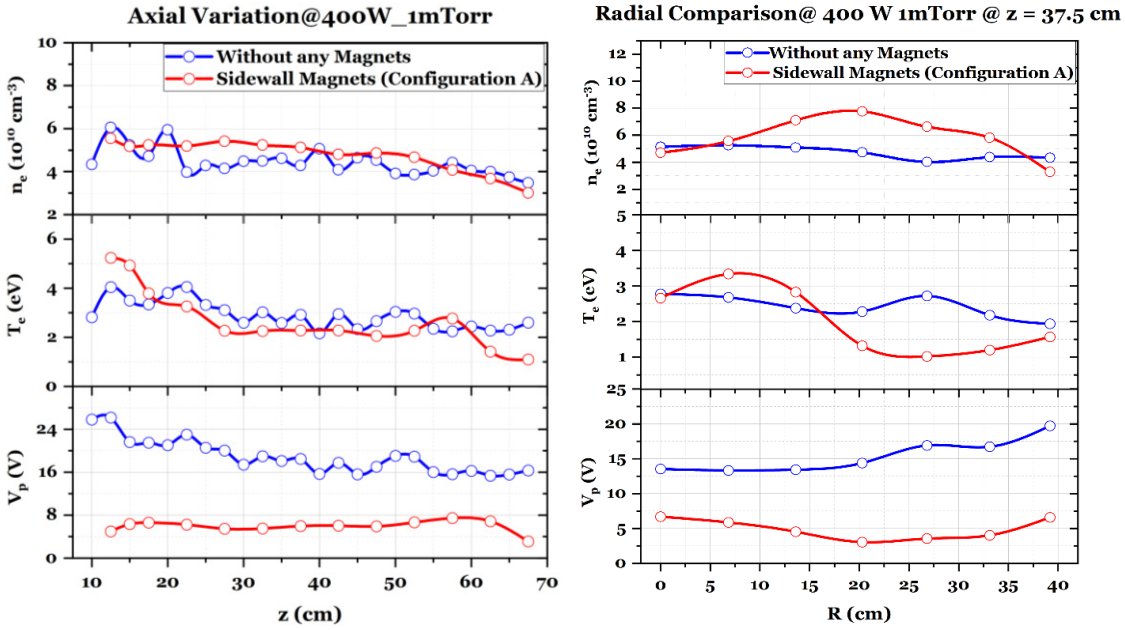

Fig 7. Axial comparison of plasma parameters (Left), Radial comparison of plasma parameters at @ z = 37.5 cm (Right) for two different magnetic field configurations.

As already mentioned, the axial magnetic field of the CEPS decays exponentially as we move away from the source and that helps in plasma flow into the expansion chamber which can be attributed to the fall in

plasma density as we move away from the source mouth axially. However, as can be seen from the vertical cross sections of the streamline plot of the magnetic field profile for configuration A in Fig 5, magnetic lines of force emerging away from the top source mouth enter the sidewall magnets placed at z = 37.5 cm that helps in the plasma flowing out of the source mouth radially which is different than that of the case with no sidewall magnets. This type of magnetic field profile inside the chamber results in reduced value of the plasma density close to the source mouth as compared to the case with no magnets and the uniformity is retained due to the cusped field of the magnets placed at the sidewall. The plasma potential is reduced significantly in presence of sidewall magnets due to reduced plasma wall losses when compared to the case without any magnets at the chamber sidewall. The radial comparison of results with two magnetic field configurations are also presented in Fig 7. From the radial measurements taken at z = 37.5 cm, one can observe that the uniformity is affected due to the presence of magnets at the sidewall. The azimuthal symmetry of the expansion chamber is disturbed due to the presence of magnets at the sidewall. However, when compared with the case having no sidewall magnets, the density is enhanced to some extent due to reduced plasma loss at the wall with sidewall cusping magnets. The same effect on plasma potential is also observed radially as seen in axial measurements in the presence of sidewall cusp configuration. In view of the fact that the density as well as the plasma uniformity is getting reduced under the current sidewall field configuration, experiments were also carried out with the second configuration B and the results are presented below.

4.2 Configuration B (*Magnets with same polarity at the sidewall*)

The experimental results obtained with the magnetic configuration – B i.e. all the magnets present at the sidewall at z = 37.5 cm have the same polarity facing the plasma as that of the top source which is south under current sets of experiment are presented. Figure 8 shows both the axial and radial variation of plasma parameters under configuration B and the comparison of the results with the case having no additional sidewall magnets are also presented. It should be noted that the radial measurements presented under this configuration B were taken with the help of RLP-1 placed at z = 37.5 cm. As anticipated from the magnetic field simulations, plasma density is getting enhanced in presence of sidewall magnets when compared to the case having no additional magnets. Enhancement in density was obtained in both axial as well as radial directions. Plasma density $n_e = 6\times10^{10}$ cm^{-3} with only top source got enhanced up to $n_e = 9\times0^{10}$ cm^{-3} due to the presence of magnets with same polarity as that of the top source that help in confining the plasma by reducing the plasm lost at the wall as in the earlier case. Comparable bulk electron temperature was obtained in both the field configurations. Reduced plasma potential and floating potential when compared to the case with no magnets present at the sidewall reflects the same. However, radial uniformity is affected which can be attributed to the disturbed azimuthal symmetry in presence of these sidewall magnets. So, there is a tradeoff between density and radial uniformity that needs further investigations. It is worth mentioning here that plasma characterizations were also performed with RLP-2 placed in between two magnets radially at z = 37.5 cm. As can be seen from Fig 5(c), due to same polarity of the magnets, a loss zone is created at the position where RLP-2 is placed. This resulted in small variations of the plasma parameters obtained with the RLP-2 probe, however, values were comparable to that of RLP-1. This variations can be further suppressed using additional magnets at the sidewall which can result in better confinement. As an alternative step towards improving the plasma uniformity, the CEPS magnets (3 concentric ring magnets) can be replaced with a single ring magnet at the sidewall. The magnetic field lines emerging from a single ring magnet penetrate less into the expansion chamber and is expected to improve the radial uniformity by pushing the cusp region close to the chamber wall. The experiments on this regard have been planned for near future.

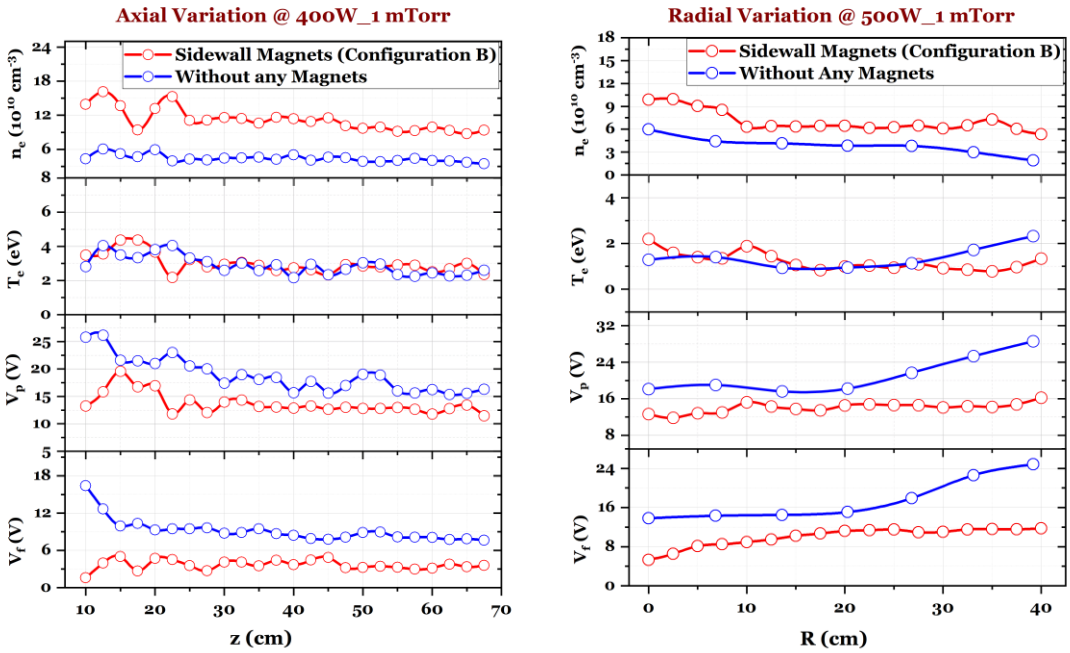

Fig 8. Axial comparison of plasma parameters (Left), Radial comparison of plasma parameters @ z = 37.5 cm (Right) for two different magnetic field configurations.

5 Conclusion

The study reports the experimental investigations carried out in a large volume plasma system with a compact ECR plasma source attached onto the top of it for plasma production, and the results obtained under two distinct chamber magnetic field configurations are presented. Axial and radial plasma parameters measured with the help of inhouse developed Langmuir probe are also presented. The results obtained with the sidewall magnets present at z = 37.5 cm in two different configurations A & B were compared with the case with no sidewall magnets. Axial variations showed moderately uniform plasma density ($n_e \sim 5\times10^{10}$ cm^{-3}) over a range of 30-35 cm at the central region of the expansion chamber with electron temperature, $T_e \sim$ 1-2 eV with sidewall magnets. When compared with the case with no magnets in the sidewall, it was observed that in configuration A, the axial density close to the source mouth is reduced due to the plasma flow towards the sidewall magnets having opposite polarity than that of the top source. As a result of this splitting, a relatively uniform axial plasma density is achieved. Electron temperature shows the same trend in both the cases with a reduced value in the presence of sidewall magnets. When compared to the case with no sidewall magnets, plasma potential is found to be reduced significantly reflecting the reduced plasma flow towards the wall resulting in a better plasma confinement due to the presence of magnets at the sidewall of the expansion chamber. Radial variation of plasma parameters reflect the enhancement in plasma density at the expense of radial uniformity which is affected in presence of sidewall magnets. In order to overcome this issue, configuration B was employed with all magnets having same polarity as that of the top source. Enhancement in plasma density was observed in both axial as well as radial direction with comparable electron temperature with slightly reduced radial uniformity were obtained with configuration B. Same effect on plasma potential and floating potential was observed as in the earlier configuration A. Overall, one can predict from these experimental results that this compact ECR plasma source can be effectively used as a

source for large area plasma applications and as an ion beam generator with further optimization. It can be tuned accordingly to be utilized in a number of applications in the field of plasma based material processing and production of ion beams for thermonuclear fusion applications.

Acknowledgements

The first author expresses gratitude to Mr. Rishabh Verma for his assistance in Langmuir probe fabrication process and conducting experiments. Authors would like to thank IPR Gandhinagar for the partial funding provided by them. The first author also acknowledges the Ministry of Education, Govt of India for providing financial support for the research endeavours.

References

1. Koui T, Suemune I, Kishimoto A, Hamaoka K H K, Yamanishi M Y M, Evaluation of hydrogenation on semiconductor surfaces treated with hydrogen-plasma beam excited by electron cyclotron resonance, *Jpn J Appl Phys*, 30(1991)3203; doi.org/10.1143/JJAP.30.3203.
2. Stavola M, Hydrogen passivation in semiconductors, *Acta Phys Pol* A, 82(1992)585–598.
3. Baert K, Murai H, Kobayashi K, Namizaki H N H, Nunoshita M N M, Hydrogen passivation of polysilicon thin-film transistors by electron cyclotron resonance plasma, *Jpn J Appl Phys*, 32(1993)2601; doi.org/10.1143/JJAP.32.2601.
4. Dong C, Patrick R E, Siminski R A, Bao T, Fluxless soldering in activated hydrogen atmosphere. In 2016 China Semiconductor Technology International Conference (CSTIC) (pp. 1-3) 2016, IEEE; doi.org/10.1109/CSTIC.2016.7464060.
5. Akatsuka F, Hirose Y, Komaki K, Rapid growth of diamond films by arc discharge plasma CVD, *Jpn J Appl Phys*, 27(1988)L1600; doi.org/10.1143/JJAP.27.L1600
6. Fojtíkova P, Radkova L, Janova D, Krcma F, Application of low-temperature low-pressure hydrogen plasma: treatment of artificially prepared corrosion layers, *Open Chem*, 13(2015)362–368.
7. Faircloth D, Lawrie S, An overview of negative hydrogen ion sources for accelerators, *New J Phys*, 20(2018) 025007; doi.org/10.1088/1367-2630/aaa39e.
8. Gamal M, El-Aragi, Ion Beam Emission within a Low Energy Focus Plasma (0.1 kJ) Operating with Hydrogen, *Z Naturforsch A*, 65(2010)606–612.
9. Stodolna A S, Mechielsen T W, van der Walle P, Meekes C, Lensen H, Novel low-temperature and high-flux hydrogen plasma source for extreme-ultraviolet lithography applications, *J Vac Sci Technol B,* 42(2024)052601; doi.org/10.1116/6.0003701.
10. James C, Williams, Martin A, Gundersen, Variable density, Uniform hydrogen plasma source for plasma-based accelerators 2017 IEEE International Conference on Plasma Science (ICOPS), Atlantic City, NJ, USA, (2017)1-1; doi.org/10.1109/PLASMA.2017.8496305.
11. Nadar R, Revolutionizing Interstellar Travel: Investigating Hydrogen and Oxygen Plasma as Cutting-Edge Rocket Propellants for Highly Efficient Thrusters, *Acceleron Aerospace Journal*, 2(2024)126–130.
12. Polushkin E A, Nefedev S V, Kovalchuk A V, Soltanovich O A, Shapoval S Y, Hydrogen Plasma under Conditions of Electron-Cyclotron Resonance in Microelectronics Technology, *Russ Microelectron*, 52(2023)195–197.
13. Speth E, Neutral beam heating of fusion plasmas, *Rep Prog Phys*, 52(1989)57; doi.org/10.1088/0034-4885/52/1/002.
14. Ikeda K, ITER on the road to fusion energy, Nuclear Fusion, 50(2010)014002; doi.org/10.1088/0029-5515/50/1/014002.
15. Chakraborty A, Rotti C, Bandyopadhyay M, Singh M J, Nair R G, Shah S, Baruah U K, Hemsworth R S, Schunke B, Diagnostic neutral beam for ITER—Concept to engineering. *IEEE Trans Plasma Sci*, 38(2009):248–253.
16. Wilhelm R, ECR Plasma Sources. In: Ferreira C M, Moisan M (eds) Microwave Discharges. NATO ASI Series, vol 302, Springer, Boston, MA(1993)8-11; doi.org/10.1007/978-1-4899-1130-8_11.
17. Fantz U, Wunderlich D, Riedl R, Heinemann B, Bonomo F, Achievement of the ITER NBI ion source parameters for hydrogen at the test facility ELISE and present Status for deuterium, *Fusion Eng Des* ,156(2020)111609; doi.org/10.1016/j.fusengdes.2020.111609.

18. Ganguli A, Tarey R D, Arora N, Narayanan R, Development and studies on a compact electron cyclotron resonance plasma source, *Plasma Sources Sci Technol*, 25(2016)025026; doi.org/10.1088/0963-0252/25/2/025026.
19. Sharma S, Sahu D, Narayanan R, Kar S, Tarey RD, Ganguli A, Bandyopadhyay M, Chakraborty A, Singh M J, Studies on Hydrogen Plasma in an ECR Based Large Volume Chamber, In 2020 IEEE International Conference on Plasma Science (ICOPS) 2020 Dec 6 (pp. 129-129). IEEE; doi.org/10.1109/ICOPS37625.2020.9717871.
20. Ganguli A, Tarey R D, 2006 Permanent Magnet Compact Electron Cyclotron Resonance Plasma Generator, Indian Patent # 301583, Patentee: IIT Delhi.
21. Plihon N, Chabert P, Corr C S, Experimental investigation of double layers in expanding plasmas, *Phys Plasmas*, 14(2007)013506; doi.org/10.1063/1.2424429.

[*Received*: 03.01.2025; *Revised recd*: 01.02.2025; *accepted*: 05.02.2025]